Since January 2020 Elsevier has created a COVID-19 resource centre with free information in English and Mandarin on the novel coronavirus COVID-19. The COVID-19 resource centre is hosted on Elsevier Connect, the company's public news and information website.

Virology 383 (2009) 291–299

Contents lists available at ScienceDirect

Virology

journal homepage: www.elsevier.com/locate/yviro

Tandem leader proteases of *Grapevine leafroll-associated virus-2*: Host-specific functions in the infection cycle

Yu-Ping Liu [a,1], Valera V. Peremyslov [a,1], Vicente Medina [b], Valerian V. Dolja [a,c,*]

[a] Department of Botany and Plant Pathology, Oregon State University, Corvallis, OR 97331, USA
[b] Department de Producio Vegetal I Ciencia Forestal de la Universitat de Lleida, Avda. Alcalde Rovira Roure 177, 25198 Lleida, Spain
[c] Center for Genome Research and Biocomputing, Oregon State University, Corvallis, OR 97331, USA

ARTICLE INFO

Article history:
Received 30 July 2008
Returned to author for revision 9 August 2008
Accepted 23 September 2008
Available online 12 November 2008

Keywords:
Papain-like protease
Closterovirus
Grapevine leafroll-associated virus-2
Systemic transport

ABSTRACT

Several viruses in the genus *Closterovirus* including *Grapevine leafroll-associated virus-2* (GLRaV-2), encode a tandem of papain-like leader proteases (L1 and L2) whose functional profiles remained largely uncharacterized. We generated a series of the full-length, reporter-tagged, clones of GLRaV-2 and demonstrated that they are systemically infectious upon agroinfection of an experimental host plant *Nicotiana benthamiana*. These clones and corresponding minireplicon derivatives were used to address L1 and L2 functions in GLRaV-2 infection cycle. It was found that the deletion of genome region encoding the entire L1–L2 tandem resulted in a ~100-fold reduction in minireplicon RNA accumulation. Five-fold reduction in RNA level was observed upon deletion of L1 coding region. In contrast, deletion of L2 coding region did not affect RNA accumulation. It was also found that the autocatalytic cleavage by L2 but not by L1 is essential for genome replication. Analysis of the corresponding mutants in the context of *N. benthamiana* infection launched by the full-length GLRaV-2 clone revealed that L1 or its coding region is essential for virus ability to establish infection, while L2 plays an accessory role in the viral systemic transport. Strikingly, when tagged minireplicon variants were used for the leaf agroinfiltration of the GLRaV-2 natural host, *Vitis vinifera*, deletion of either L1 or L2 resulted in a dramatic reduction of minireplicon ability to establish infection attesting to a host-specific requirement for tandem proteases in the virus infection cycle.

Introduction

Diverse RNA and DNA viruses of eukaryotes rely on proteases for the needs of genome expression and virus–host interactions (Barrett and Rawlings, 2001; Dougherty and Semler, 1993; Koonin and Dolja, 1993; Lindner, 2007). The several distinct classes of the viral proteases appear to have evolved independently following acquisition of the related enzymes of the host cells with the chymotrypsin-like proteases (3C proteases) of picona-like viruses being a prime example (Gorbalenya et al., 1989). Another class of widespread viral proteases is papain-like proteases present in diverse families of the positive-strand RNA viruses (Gorbalenya et al., 1991). Independent of their evolutionary origins, viral proteases can be subdivided into the categories of main and leader proteases. The main proteases typified by the picornaviral 3C-protease are responsible for multiple cleavages within the viral polyprotein. In contrast, leader proteases are typically located at the N-terminus of the polyprotein and cleave *in-cis* only at their own C-termini. A well-studied example of a leader protease is an eponymous protease of the animal aphtoviruses (de los Santos et al., 2006). Interestingly, several diverse viral groups, e.g., animal nidoviruses (Ziebuhr et al., 2000) and plant potyviruses (Urcuqui-Inchima et al., 2001) possess two leader proteases arranged in a tandem.

In addition to self-processing, many leader proteases are required for efficient amplification or transcription of the viral genome. In particular, nsp1 papain-like protease of arteriviruses regulates synthesis of the subgenomic mRNAs (Tijms et al., 2007), while the potyviral papain-like protease HC-Pro is required for efficient genome accumulation (Kasschau et al., 1997). Another common theme in the functions of leader proteases is virus–host interactions. Thus, aphtoviral leader protease facilitates viral infection by interfering with regulation of the host protein synthesis and innate immune response (de los Santos et al., 2006). The papain-like proteases of the potyviruses and fungal hypoviruses are the potent suppressors of the antiviral RNA interference (RNAi) response (Ding and Voinnet, 2007; Lakatos et al., 2006; Segers et al., 2006). The fact that in different potyviruses either papain-like or chymotrypsin-like protease can assume the RNAi suppression function (Valli et al., 2006) highlights the evolutionary plasticity of the leader proteases. Indeed, many of these proteases contain additional domains such as insect transmission (Ng and Falk, 2006) or RNA demethylase

* Corresponding author. Fax: +1 541 737 3573.
E-mail address: doljav@science.oregonstate.edu (V.V. Dolja).
[1] These two authors contributed equally to this work.

0042-6822/$ – see front matter © 2008 Elsevier Inc. All rights reserved.
doi:10.1016/j.virol.2008.09.035

(Susaimuthu et al., 2008; van den Born et al., 2008) domains found in papain-like and chymotrypsin-like proteases, respectively, of the distinct potyviruses.

Closteroviruses possess the largest genomes among all known plant viruses and belong to the alphavirus-like superfamily of the positive-strand RNA viruses (Koonin and Dolja, 1993). The family Closteroviridae contains three genera defined on the basis of phylogenetic analysis, genome organization, and the type of the vectoring insects (Dolja et al., 2006; Karasev, 2000). In particular, genus *Closterovirus* with *Beet yellows virus* (BYV) as a prototype member (Dolja, 2003) contains the aphid-transmissible viruses with the 15–20 kb, monopartite genomes. Similar to other family members, BYV encodes a papain-like leader protease (L-Pro), RNA replicase (Peng et al., 2001; Peremyslov et al., 1998), and a quintuple block of genes responsible for virion assembly and cell-to-cell movement (Alzhanova et al., 2000, 2001, 2007; Peremyslov et al., 1999; Peremyslov et al., 2004b). In addition, BYV encodes a RNAi suppressor that is conserved in this genus (Chiba et al., 2006; Lu et al., 2004; Reed et al., 2003), and a 20-kDa long-distance transport factor (p20) (Prokhnevsky et al., 2002).

Perhaps, the most conspicuous feature of closteroviruses is the complex molecular architecture of their exceptionally long filamentous virions. These virions contain an over 1000 nm-long 'body' assembled by the major capsid protein (CP) and a ~100 nm-long 'tail' whose major component is a minor capsid protein (CPm) (Agranovsky et al., 1995) evolutionary related to CP (Boyko et al., 1992). Tails encapsidate ~700 nt-long, 5′-terminal region of the virion RNA (Alzhanova et al., 2007; Peremyslov et al., 2004a, 2004b; Satyanarayana et al., 2004). In addition to CPm, tails incorporate the Hsp70 homolog and ~60-kDa protein (Napuli et al., 2003; Napuli et al., 2000; Peremyslov et al., 2004a, 2004b; Satyanarayana et al., 2000; Tian et al., 1999) that facilitate tail assembly by CPm and define the tail length (Alzhanova et al., 2007; Satyanarayana et al., 2004). In BYV, tail exhibits a three-segment structure with the tip segment likely formed by the long-distance transport factor p20 (Peremyslov et al., 2004a). Because the mutant tail-less virions formed by CP alone are capable of encapsidating the entire genome (Alzhanova et al., 2001; Satyanarayana et al., 2004), and because each tail component is essential for virus transport (Alzhanova et al., 2000; Peremyslov et al., 1999; Prokhnevsky et al., 2002), tail apparently evolved as a device for facilitating *Closterovirus* spread in the infected plants (Dolja et al., 2006). Strikingly, tail-like structures potentially involved in virion transport were also discovered in potyviruses (Gabrenaite-Verkhovskaya et al., 2008; Torrance et al., 2005).

Our previous work showed that the BYV L-Pro is required for efficient RNA amplification and virus long-distance transport (Peng et al., 2003; Peng and Dolja, 2000). Interestingly, replacement of L-Pro by the proteases from other closteroviruses (Peng et al., 2001) or even from an animal arterivirus (Peng et al., 2002) can rescue the RNA amplification, but not the transport function of the leader protease. It seems likely that the role of L-Pro in systemic transport is dual. First, it has a specific, protein-mediated role that was revealed by the site-directed mutagenesis (Peng et al., 2003). Second, because tail encapsidates the 5′-terminal one third of the protease-coding region, mutations in this area can interfere with the tail assembly and virus transport.

The *Grapevine leafroll-associated virus-2* (GLRaV-2) is a close BYV relative in the *Closterovirus* genus whose genetic organization is almost identical to that of BYV (Zhu et al., 1998). However, unlike BYV that possesses one leader protease, GLRaV-2 codes for two leader proteases, L1 and L2 (Meng et al., 2005; Peng et al., 2001) (Fig. 1A, top diagram). Here we demonstrate that L1 and L2 have complementary functions in establishment of the GLRaV-2 infection in the initially inoculated cells and systemic transport. Strikingly, overall contribution of L1 and L2 into virus infection is much more critical in a natural virus host, grapevine, compared to an experimental herbaceous host, *Nicotiana benthamiana*, suggesting that the tandem of leader proteases evolved to facilitate an expansion of the *Closterovirus* host range.

Results

Generation of GLRaV-2 replicons tagged by insertion of the fluorescent, enzymatic, and epitope reporters

Because the infectious cDNA clones provide powerful tools for investigation of the RNA virus gene functions (Peremyslov and Dolja, 2007; Pogue et al., 2002), we generated such clone for GLRaV-2 to determine functional profiles of L1 and L2. The entire, 16,486 nt-long GLRaV-2 genome was sequenced (Genbank accession no. FJ436234) and compared to the other isolates of this virus to reveal the closest relationship (99.6% nt identity) to the isolate 94/970 (Meng et al., 2005). The initial full-length clone was assembled using a binary vector and primarily conventional cDNA cloning to avoid introduction of the PCR-generated mutations, and sequenced to confirm its correspondence to the consensus nucleotide sequence of the viral genome. To facilitate launching of viral infection by agroinoculation, 35S RNA polymerase promoter of *Cauliflower mosaic virus* (CaMV) and a ribozyme sequence were inserted upstream and downstream of the GLRaV-2 sequence, respectively, as described earlier for BYV (Peremyslov and Dolja, 2007; Prokhnevsky et al., 2002).

The resulting full-length GLRaV-2 clone was further modified to accommodate a reporter gene expression cassette immediately upstream of the CP open reading frame. This cassette contained GFP open reading frame followed by the BYV CP subgenomic RNA promoter. As a result, the latter promoter directed expression of the GLRaV-2 CP, while the authentic GLRaV-2 CP promoter expressed the GFP reporter. This tagged full-length GLRaV-2 replicon was designated LR-GFP (Fig. 1A, middle diagram).

As was shown for BYV, deletion of the genes that are not required for the viral RNA amplification in the individual cells facilitates experimentation with the remaining genes that code for the leader protease, RNA replicase and RNAi suppressor (Chiba et al., 2006; Hagiwara et al., 1999; Peng and Dolja, 2000). In the case of GLRaV-2, such minireplicon was generated by deletion of the gene block spanning genome region from p6 to p19 open reading frames and retention of the reporter gene. The reporter expression cassette was further modified to express a fusion of GFP with β-glucuronidase to result in the tagged GLRaV-2 minireplicon designated mLR-GFP/GUS (Fig. 1A, bottom diagram).

To permit immunochemical detection of L2, both LR-GFP and mLR-GFP/GUS were modified by an insertion of the triple hemagglutinin epitope (HA) tag into the N-terminal domain of L2 ($L2_{HA}$ in the Figs. 1B and 2). Infectivity of the full-length and minireplicon variants was tested using leaf agroinfiltration of *N. benthamiana*, a systemic experimental host of GLRaV-2 (Goszczynski et al., 1996). For mLR-GFP/GUS, such agroinfiltration resulted in minireplicon RNA accumulation and efficient expression of the fluorescent and enzymatically-active GFP/GUS reporter in the initially inoculated cells (Fig. 1B and data not shown). Importantly, the level of GUS activity in a HA-tagged variant was ~85% of that in the original mLR-GFP/GUS. Because this modest reduction was only marginally statistically significant (p value ~0.001), we concluded that the insertion of HA tag into L2 did not significantly affect viral genome amplification. Our attempts to insert an HA tag into L1 resulted in non-infectious replicons and were abandoned.

Both the original and HA-tagged variants of the full-length LR-GFP were systemically infectious in *N. benthamiana*; typical symptoms of the viral infection and GFP fluorescence were detected in the upper non-inoculated leaves by 3 weeks post-agroinfiltration of the bottom leaves (Fig. 1A and data not shown). Therefore, we successfully generated a series of the infectious tagged GLRaV-2 replicons that can

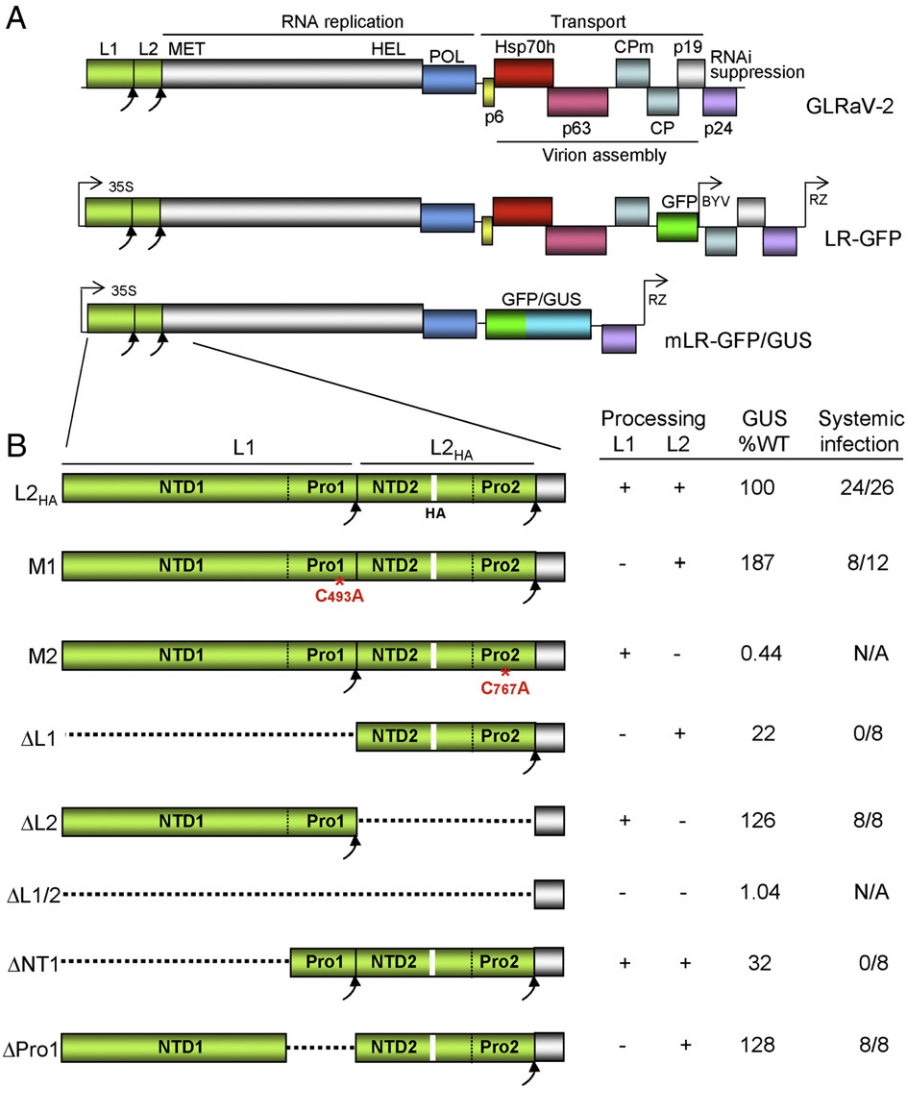

Fig. 1. (A) Diagrams of GLRaV-2 genome (top), full-length, GFP-tagged cDNA clone of GLRaV-2 (LR-GFP, middle) and GFP/GUS-tagged minireplicon (mLR-GFP/GUS, bottom). Functions of viral genes are shown above and below the diagram. L1 and L2, leader proteases; MET, HEL, and POL, methyltransferase, RNA helicase, and RNA polymerase domains, respectively; p6, 6-kDa movement protein; Hsp70h, Hsp70 homolog; p63, 63-kDa protein; CPm, minor capsid protein; CP, major capsid protein; p19, 19-kDa protein; p24, 24-kDa protein; GFP, green fluorescent protein; GFP/GUS, GFP fusion with β-glucuronidase; 35S, 35S RNA polymerase promoter of *Cauliflower mosaic virus*; RZ, ribozyme. (B) Diagrams of the mutations introduced into L1 and L2 (left) and corresponding phenotypes indicating processing activity, levels of GUS expression, and systemic infectivity. $L2_{HA}$, insertion of the triple hemagglutinin epitope into L2 (HA, white strip); M1, replacement of the L1 catalytic Cys residue with Ala ($C_{493}A$); M2, replacement of the L2 catalytic Cys residue with Ala ($C_{767}A$); ΔL1, deletion of the entire L1 coding region; ΔL2, deletion of the entire L2 coding region; ΔL1/2, deletion of the entire L1 and L2 coding regions; ΔNT1, deletion of the region encoding N-terminal, non-proteolytic domain of L1; ΔPro1, deletion of the region encoding C-terminal, proteolytic domain of L1.

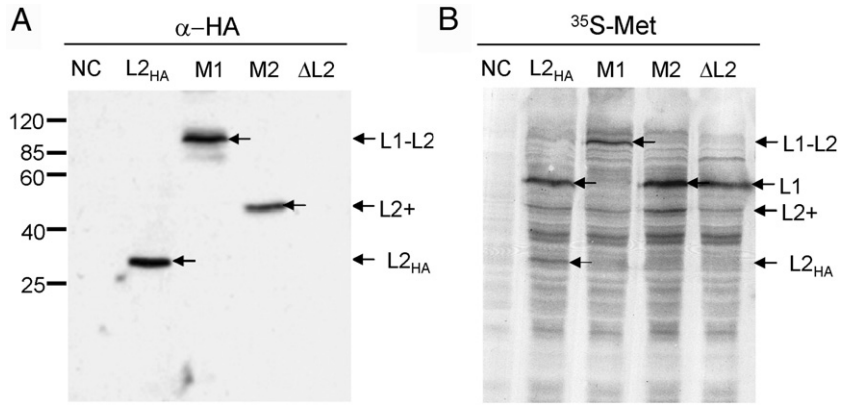

Fig. 2. L1- and L2-mediated processing of the N-terminal part of the GLRaV-2 polyprotein generated *in vitro*. Lanes correspond to mutant variants shown in the Fig. 1B except for NC, no RNA control. (A) Immunoblot analysis of the *in vitro* translation products using HA-specific antibody (α-HA) to detect L2. Arrows at the right mark the following processing products: L1–L2, unprocessed fusion of L1 and L2; L2+, L2 fused to a part of MET; $L2_{HA}$, fully processed, HA-tagged L2. Numbers at the left show the mol. mass (kDa) of the protein markers. (B) Analysis of the ^{35}S-methyonine-labeled *in vitro* translation products. Designations are as in (A).

be launched to *N. benthamiana* and used to address L1 and L2 functions in the viral infection cycle.

Mutation analysis of the L1 and L2 functions in protein processing and RNA accumulation in the initially inoculated cells of N. benthamiana

To address L1 and L2 functions, seven point mutations and deletions were introduced into corresponding coding region (Fig. 1B). In particular, to determine the requirements for the self-processing at the respective C-termini of L1 and L2, the predicted catalytic cysteine residues of the each protease (Cys_{493} and Cys_{767}) (Peng et al., 2001) were replaced by alanine residues to result in M1 and M2 variants, respectively (Fig. 1B). The processing competence of each variant was investigated using *in vitro* translation of the capped mRNAs encompassing the 5′-terminal untranslated region, the entire L1–L2 open reading frame and a short downstream region that encodes a part of the methyltransferase domain (Fig. 1B). The resulting translation products were analyzed using either immunoblotting and HA-specific antibody (Fig. 2A) or ^{35}S-methionine labeling (Fig. 2B). As expected, a tagged non-mutant variant produced single HA-positive band corresponding to the fully-processed, HA-tagged L2 (Fig. 1B and Fig. 2A, lane $L2_{HA}$) and, in addition, isotope-labeled, fully processed L1 (Figs. 1B and 2B, lane $L2_{HA}$).

In contrast, translation of the M1 variant resulted in accumulation of a single major product corresponding to a L1–L2 fusion (Fig. 1B; Figs. 2A and B, lanes M1). Analogously, mutational replacement of the predicted catalytic cysteine in L2 resulted in a lack of L2 self-processing, but did not affect the autocatalytic release of L1 (Fig. 1B; Figs. 2A and B, lanes M2). Because mutation of the predicted active site residues did inactivate autoproteolysis by each leader protease, we concluded that L1 and L2 are indeed the catalytically active, papain-like proteases.

To determine if the processing by L1 and L2 is required for viral RNA amplification, we used M1 and M2 variants of mLR-GFP/GUS to agroinfiltrate *N. benthamiana* leaves and to determine the resulting GUS activity. As shown previously for BYV minireplicon, GUS activity provides a reliable surrogate marker for measuring accumulation of the viral RNAs in the infected cells (Peng and Dolja, 2000). Using this marker, we found that, unexpectedly, inactivation of the L1 cleavage resulted in more efficient GUS expression; almost 2-fold increase in GUS activity was detected in three independent experiments (Fig. 1B). In contrast, inactivation of L2 cleavage virtually abolished minireplicon infectivity: the corresponding GUS expression level was less than 0.5% of that of the parental mLR-GFP/GUS (Fig. 1B). This result is in complete agreement with the strict requirement for the cleavage by L-Pro for BYV minireplicon infectivity (Peremyslov et al., 1998); indeed fusion of either L-Pro or L2 with the replicase is likely to interfere with the synthesis of viral RNAs.

To further define the roles of L1 and L2 in RNA accumulation, we have generated the mutants in which the coding regions of L1, L2, or both, were deleted. Interestingly, the L1 null mutant ΔL1 was capable of replication, although a corresponding level of GUS activity was ~5-fold lower than that in the parental mLR-GFP/GUS variant (Fig. 1B). Unexpectedly, deletion of L2 in the ΔL2 variant resulted in a slight increase in GUS expression suggesting that L2 is not essential for minireplicon accumulation in the *N. benthamiana* cells (Fig. 1B). However, simultaneous deletion of L1 and L2 yielded the minireplicon ΔL1/2 that expressed only ~1% of the GUS activity observed in a parental mLR-GFP/GUS variant (Fig. 1B). Taken together, these results indicated that although the role of L1 in viral RNA amplification is more prominent than that of L2, the latter protease can rescue RNA accumulation of the L1-deficient mutant, and therefore L1 and L2 have partially overlapping functions in this process.

Both L1 and L2 possess the C-terminal papain-like protease domains (Pro1 and Pro2, respectively) and the N-terminal domains (NTD1 and NTD2, respectively; Fig. 1B). To determine the relative contributions of NTD1 and Pro1 in the L1 function, we generated ΔNTD1 and ΔPro1 variants in which these domains were deleted (Fig. 1B). The former of these minireplicon variants exhibited ~3-fold reduction in accumulation of GUS, while the latter produced even more GUS than the parental variant (Fig. 1B). These data indicated that the non-proteolytic rather than the protease domain of L1 provides a major contribution to viral RNA accumulation in *N. benthamiana* cells. It should be emphasized that the observed requirement for NTD1 for optimal RNA accumulation can reflect either a role of a protein domain, or of a corresponding coding region at the RNA level, or both.

Roles of L1 and L2 in the virion infectivity and systemic spread of GLRaV-2 in N. benthamiana

To define the potential functions of L1 and L2 in the viral cell-to-cell movement and long-distance transport, the ΔL1 and ΔL2 deletions were introduced into the background of the full-length LR-GFP variant. Following agroinfiltration, virions were isolated from the inoculated leaves and the virion suspensions of the equal concentrations were used to manually inoculate *N. benthaniana* leaves and to characterize the resulting infection foci using GFP fluorescence at 8 days post-inoculation (Peremyslov et al., 1999). For the parental LR-GFP variant, inoculation yielded 9.9±5.6 infection foci per leaf with the mean diameter of 4.3±1.4 cells. Very similar results (8.2±4.8 foci per leaf; mean diameter of 4.1±1.3 cells) were obtained for the LR-GFPΔL2 variant indicating that L2 is dispensable for both the infectivity and cell-to-cell movement of the GLRaV-2 in *N. benthamiana*. Strikingly, deletion of L1 resulted in a dramatic, 25-fold reduction in the specific infectivity of the LR-GFPΔL1 variant (0.4 cells per leaf). Furthermore, the very few detected GFP-positive foci were unicellular suggesting that either L1 or the corresponding coding region is essential for the virion ability to establish infection in the initially inoculated cells and to move to the neighboring cells.

To determine if L1 and L2 are involved in the systemic transport of GLRaV-2, we tested six replication-competent variants in a context of the full-length LR-GFP launched to *N. benthamiana* plants using agroinfiltration. The inoculated plants were screened for the symptom, GFP, and CP expression at 3, 4, and 5 weeks post-inoculation. Interestingly, most or all of the plants inoculated with M1 and ΔL2 variants became systemically infected indicating that neither L2 nor the cleavage between L1 and L2 is required for the long-distance transport of the virus in *N. benthamiana* (Figs. 1B and 3A). Similar competence for the systemic spread was found in the case of ΔPro1 mutant. However, deletion of the L1 or its N-terminal domain resulted in complete loss of the replicon ability to establish systemic infection (Figs. 1B and 3C).

Observation of the systemically infected leaves revealed apparent differences in the GFP accumulation between the experimental variants (Fig. 1A). To further assess these differences, we evaluated GLRaV-2 CP accumulation in the non-inoculated upper leaves. Conspicuously, it was found that only the ΔPro1 mutant accumulated to the levels comparable to those of the parental $L2_{HA}$ variant (Fig. 3B). The remaining two mutant variants, M1, and especially ΔL2, each accumulated to the significantly lower levels than that of the parental LR-GFP variant both at 3 and 4 weeks post-inoculation (Fig. 3B). Collectively, these results demonstrated that the L2 per se, and the cleavage between L1 and L2 are required for optimal systemic spread of GLRaV-2 in *N. benthamiana*. In addition, L1 and its N-terminal non-proteolytic domain or the corresponding coding regions are essential for the ability of GLRaV-2 to establish systemic infection since neither GFP nor viral CP were detectable in the upper leaves of the plants inoculated with the ΔNTD1 or ΔL1 variants even at 5 weeks post-inoculation (Fig 3C and D).

In BYV, both p20 and L-Pro are involved into viral systemic spread (Peng et al., 2003; Prokhnevsky et al., 2002). Of these, p20 is an integral component of the virion tail (Peremyslov et al., 2004a, 2004b),

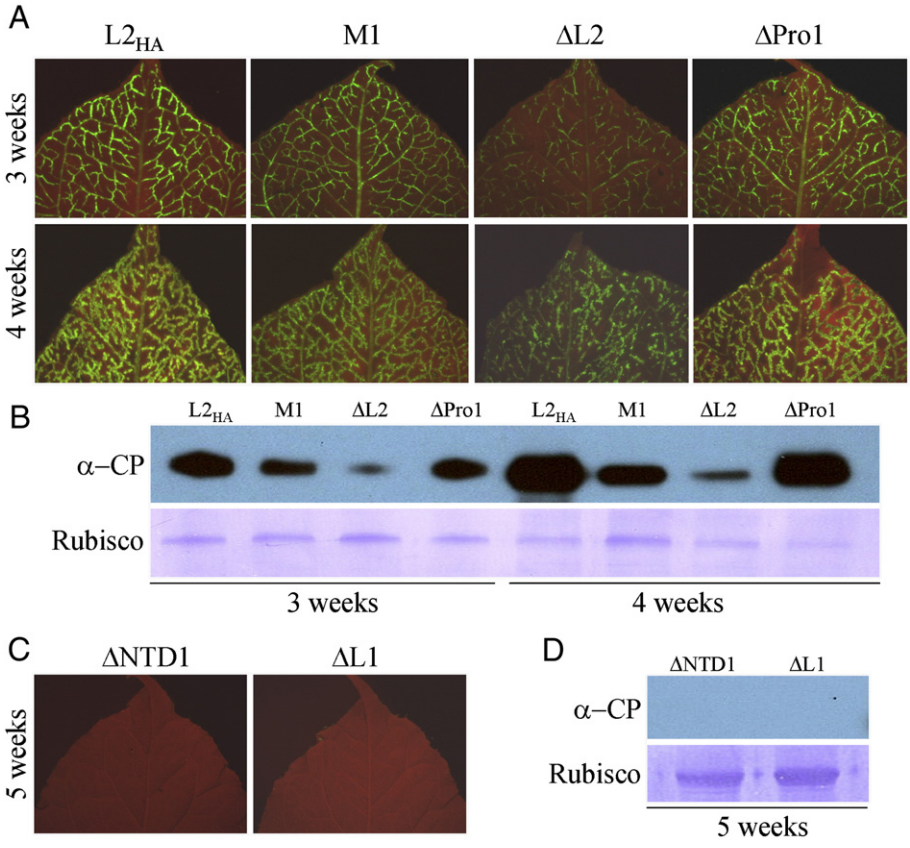

Fig. 3. Systemic transport of the LR-GFP variants harboring HA-tagged L2 following agroinoculation of *N. benthamiana*. Variants are marked as in Fig. 1B. (A) Images of the upper, non-inoculated leaves under epifluorescent stereoscope showing GFP expressed in veins. (B) Immunoblot analyses using anti-CP antibody (α-CP, top). Bottom panel, loading control showing Coomassie-stained Rubisco band on the membrane used for immunoblotting. (C and D) Lack of systemic infection in the plants agroinoculated using ΔNTD1 and ΔL1 variants revealed using epifluorescent microscopy (C) or immunoblotting (D).

while it is not known if L-Pro is present in the virions due to unavailability of the L-Pro-specific antibody. Because we generated functional, HA-tagged variant of L2, we were interested to determine if this protease is associated with the virions. The GLRaV-2 virions were isolated from systemically infected leaves and fractionated using sucrose density gradient. The peak of virions was detected in fractions 12–14 using CP-specific antibody (Fig. 4). However, the immunoblot analysis of the same gradient fractions using HA-specific antibodies showed the peak of L2 in fractions 15–17, suggesting that L2 present in the virion suspension is not physically associated with the virions (Fig. 4). This conclusion was further supported by the immunogold-specific electron microscopy used to detect HA epitopes present in L2. Indeed, only very weak gold labeling was found in the fractions 12–14 that contained bulk of the virions. Furthermore, a few gold microspheres detected in these fractions were not directly associated with the virions (Fig. 4, upper inset). The L2 peak fractions 15–17 contained much larger numbers of gold microspheres, but virtually no virions (Fig. 4, bottom inset) suggesting that L2 is not directly associated with GLRaV-2 virions.

L1 and L2 are critical for minireplicon infection of the Vitis vinifera

It is generally accepted that *N. benthamiana* is, perhaps, the most promiscuous host for a great variety of plant viruses (Goodin et al., 2008). To determine if the seemingly non-essential and largely redundant roles played by L1 and L2 in GLRaV-2 infection in this experimental host do faithfully reflect their roles in a grapevine infection, we agroinfiltrated four minireplicon variants to *V. vinifera* (Grenache) leaves (Table 1). At 8 days post-inoculation with the parental mLR-GFP/GUS variant, up to ~300 unicellular, GFP-

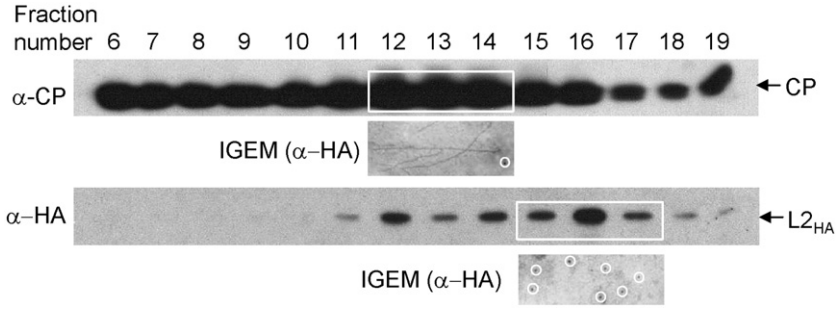

Fig. 4. Sucrose density gradient separation and immunoblot analysis of the GLRaV2 virions using anti-CP antibody (α-CP, top) or anti-HA antibody (α-HA, bottom). Gradient fractions were numbered from the bottom of the gradient. The insets show HA-specific immunogold electron microscopy analysis (IGEM) of the combined fractions marked by white boxes; white circles highlight gold microspheres. Arrows mark positions of L2-Pro and CP.

Table 1
Infectivity and GUS expression by mLR-GFP/GUS minireplicon variants in *V. vinifera*

Experiment	Variant	Mean number of the infection foci (% of that in parental variant)	Mean GUS activity (% of the level in parental variant)
1	mLR-GFP/GUS	100.00	100.00
1	ΔL1	1.03	4.16
1	ΔL2	14.96	10.03
1	M1	104.44	103.11
2	mLR-GFP/GUS	100.00	100.00
2	ΔL1	1.58	2.93
2	ΔL2	10.44	10.87
2	M1	133.43	118.08

fluorescent infection foci per leaf were observed. Strikingly, infiltration using ΔL1 and ΔL2 variants resulted in a ~100-fold and ~7-fold reduction in the foci numbers, respectively, indicating that each of the leader proteases is required for the ability of minireplicon to establish infection in the initially inoculated grapevine leaf cells (Table 1). However, similar to what was observed in *N. benthamiana*, infectivity of the M1 variant was not significantly different from that of the parental variant.

Remarkably, measurements of GUS activity in the infiltrated leaves correlated well with the data on the numbers of the infected cells (Table 1) suggesting that the principal function of the leader proteases is to aid the establishment of viral infection rather than to increase accumulation of viral RNA in the infected cells. Because the effects of L1 and L2 deletion in *V. vinifera* were much more dramatic compared to those in *N. benthamiana*, we suggest that each protease provides a significant and specific contribution into establishment of GLRaV-2 infection in its natural host plant. It should be noted, however, that our experimental design is based on agroinfiltration and targets the leaf epidermal and mesophyll cells whereas in the natural grapevine infections, GLRaV-2 is generally limited to the phloem.

Discussion

Previous work suggested that the tandems of the leader proteases in different closteroviruses emerged via independent gene duplication events (Peng et al., 2001). It was also proposed that the evolution of L1 and L2 involved functional divergence (neofunctionalization) that resulted in the erosion of sequence similarity in the corresponding N-terminal domains. By and large, an experimental analysis presented here corroborated these assumptions and allowed us to delineate three major functions of L1 and L2 in the GLRaV-2 infection cycle: i) polyprotein processing; ii) virus accumulation in the initially infected cells; iii) systemic transport of the infection.

In particular, we found that both L1 and L2 are the active proteases with the conserved catalytic cysteines (Figs. 1B and 2). Similar to BYV, the cleavage upstream from the methyltransferase domain of the viral polyprotein is essential for GLRaV-2 viability (Fig. 1B) (Peremyslov et al., 1998). Surprisingly, although L1 does cleave at its own C-terminus both *in vitro* (Fig. 2) and *in vivo* (Fig. 4), neither this cleavage nor the L1 protease domain per se are essential for systemic infection in *N. benthamiana* as evident from the phenotypes of M1 and ΔPro1 variants (Figs. 1B and 3). However, slower virus accumulation in the non-inoculated leaves in these mutants (Figs. 3A and B) suggests that the L1-mediated cleavage is required for the optimal development of systemic infection.

Our deletion analysis indicated that L1 and L2 play partially overlapping roles in the viral RNA accumulation. When viral minireplicon was launched by agroinfiltration, complete deletion of L1 resulted in a ~5-fold reduction in RNA levels. Similar effect was observed upon deletion of the N-terminal domain of L1 indicating its principal role in L1 function (Fig. 1B). Although the deletion of L2 did not affect RNA accumulation, combined deletion of L1 and L2 resulted in a virtually nonviable minireplicon attesting to a significant contribution of L2 into viral infectivity in the absence of L1.

Interestingly, when isolated virions containing full-length genome were used for plant inoculation, the infectivity and cell-to-cell movement of the ΔL2 variant were indistinguishable from those of the parental variant, while the virions of ΔL1 variant have lost their infectivity. Because both in BYV and in CTV, the 5′-terminal, ~700 nucleotide-long region is involved in the assembly of virion tails (Peremyslov et al., 2004a, 2004b; Satyanarayana et al., 2004), we assume that this region plays a similar role in GLRaV-2. If so, the deletion of L1 coding region could affect virion structure, stability, and infectivity. Therefore, we propose that in addition to L1 involvement in RNA accumulation, the corresponding coding region also functions at the RNA level to facilitate formation of the tailed virions capable of the local and systemic transport.

In accord with the latter assumption, ΔL1 and ΔNTD1 mutants were unable to establish a systemic infection upon agroinfiltration using full-length replicons (Fig. 3C). In contrast, deletion of the protease domain in ΔPro1 variant did not affect systemic infectivity indicating that virion tail formation was likely unaffected. The deletion of L2 resulted in a systemically infectious ΔL2 variant, which, however, exhibited slower accumulation in the upper leaves (Figs. 2A and B). This result indicated that L2 is required for the efficient systemic spread of GLRaV-2 in *N. benthamiana*.

Perhaps the most significant results of this study were obtained when the minireplicon variants were agroinoculated to the grapevine leaves. In a sharp contrast to *N. benthamiana* where L2 was superfluous for minireplicon infectivity, ΔL2 variant exhibited a ~10-fold reduction in RNA accumulation upon agroinfiltration into *V. vinifera* leaves (Table 1). The specific infectivity of the ΔL2 variant measured as a mean number of the GFP-fluorescent infected cells per leaf was also reduced ~10-fold. This correlation in the RNA accumulation and the numbers of infected cells points to a role of L2 in the virus invasiveness, i.e., the ability to establish infection in the inoculated cells. Such role in GLRaV-2 invasiveness in grapevine is even more dramatic in the case of L1 where L1 deletion resulted in ~100-fold reduction in the RNA accumulation and specific infectivity (Table 1). We concluded that both L1 and L2 are essential for the ability of GLRaV-2 to establish infection in the initially inoculated grapevine cells, at least upon the conditions of agroinfection.

Because M1 variant was identical to the parental minireplicon variant in its infectivity in grapevine, it appears that, similar to results obtained in *N. benthamiana*, cleavage between L1 and L2 is not essential for virus infection of the initially inoculated cells. Interestingly, a similar pattern of cleavage requirements was found in a human coronavirus where the proteolytic activity of the papain-like protease $PL2^{pro}$ was essential for virus infection while that of $PL1^{pro}$ was not (Ziebuhr et al., 2007). Taken together with partial functional overlap between the BYV L-Pro and arteriviral nsp1 (Peng et al., 2002), these striking analogies among diverse viruses suggest parallel requirements for evolution of the large RNA genomes (Dolja et al., 2006; Gorbalenya et al., 2006; Koonin and Dolja, 2006).

What is a functional significance of duplication of the leader proteases in GLRaV-2? We hypothesize that the answer, at least in part, lies in the host-specific effects of L1 and L2 whose functional cooperation is more important for the infection of grapevine than *N. benthamiana*. A tandem of viral proteases could have evolved to boost the function of a single protease in order to subvert a perennial woody host potentially recalcitrant to virus infection. This hypothesis is compatible with the fact that in addition to GLRaV-2, protease duplication is found in CTV (Karasev et al., 1995), *Raspberry mottle virus* (Tzanetakis et al., 2007), and *Strawberry chlorotic fleck virus* (Tzanetakis and Martin, 2007), each of which infects woody and/or perennial hosts, but not in BYV or *Mint virus 1* (Tzanetakis et al., 2005) that infect herbaceous annual hosts. Another example of a viral protein that apparently evolved to allow the viral infection of the woody or

perennial hosts is provided by the AlkB demethylase found primarily in a subset of flexiviruses (Martelli et al., 2007; van den Born et al., 2008).

The generation of the GLRaV-2 variants tagged via insertion of the reporter genes or epitopes highlights a potential of this virus as a gene expression vector for the grapevine. In general, *Closterovirus*-derived vectors provide advantages of relatively large genetic capacity and stability (Dolja et al., 2006; Folimonov et al., 2007). Utility of closteroviral vectors is further enhanced by a dramatic increase in the vector infectivity by co-expression of the homologous RNAi suppressors with p24 of GLRaV-2 being among the strongest (Chiba et al., 2006). Obviously, full realization of the GLRaV-2 vector potential requires development of the efficient inoculation technique for the grapevine.

Materials and methods

Generation of the GFP-tagged, full-length cDNA clone of GLRaV-2

The GLRaV-2 isolate obtained from a local Oregonian vineyard was propagated on *N. benthamiana* plants as described earlier (Goszczynski et al., 1996). Virions were isolated (Napuli et al., 2000) and the viral RNA was obtained using TRIzol reagent (Invitrogen) according to the manufacturer's protocol. A strategy for nucleotide sequencing of the viral genome and the generation of the intermediate and full-length viral cDNA clones was as described for BYV (Peremyslov and Dolja, 2007). The resulting sequence of GLRaV-2 RNA was deposited to Genbank (accession no. XXXX). The sequences of the numerous primers used in cloning procedures are available upon request.

In brief, a full-length cDNA clone of GLRaV-2 was assembled using pCB301 mini-binary vector (Xiang et al., 1999), while the cDNA cloning was done using reverse transcription and either conventional synthesis of a double-stranded (ds) cDNA or PCR amplification. The NOS terminator was added to the pCB301 by using unique sites Sac I and Kpn I and a polylinker containing restriction sites Sac I, Bam HI, AatI I, Bbvc I, Rsr II, Bst EII, and Sma I was inserted between Sac I site and NOS terminator to produce pCB301-NOS-PL. To add a CaMV 35S RNA polymerase promoter fused to the 5′-fragment of the viral cDNA (nts 1–2034), a PCR-mediated DNA splicing technique was used. Separate PCRs were done to amplify the 35S promoter and the 5′end of GLRaV2 cDNA and to generate products with overlapping ends. These products were combined and used as templates for another round of PCR using primers complementary to the 5′- and 3′-ends of the full-length product. The latter product was cloned into pCB301-NOS-PL using Sac I (added to the 5′-end of 35S promoter) and BamH I (nt 2034) to produce p35S5′LR.

To add a ribozyme to the 3′-end of the viral cDNA, a megaprimer with a virus-specific part complementary to the 3′-end of the viral cDNA followed by a ribozyme sequence designed as described (Prokhnevsky et al., 2002) and a Sma I site was used in combination with a regular primer to amplify the 3′-terminal region of the GLRaV-2 cDNA (nts 14,842–16,486). Resulting PCR product was cloned into p35S5′LR using restriction sites BstE II (nt 14,842) and Sma I (added at the 3′-terminus of the megaprimer) to produce a p35S5′3′LR-Rib.

For cloning the internal region of viral cDNA (nts 2029–10,827), three partially overlapping fragments of ds cDNA were obtained using conventional cDNA cloning and Gibco-BRL protocol for SuperScript II reverse transcriptase. These fragments were inserted into p35S5′3′LR-Rib using restriction sites Bam HI (nt 2029), Aat II (nt 3394), Bbv CI (nt 6281), and Rsr II (nt 10,821) to generate p35S-5′BR3′LR-Rib. The remaining part of the viral cDNA (nts 10,821-14,848) was PCR-amplified and cloned into an intermediate vector pGEM-3Zf(+) (Promega). A nucleotide sequence encoding an endoplasmic reticulum-targeted GFP (Haseloff et al., 1997) followed by a BYV CP promoter was inserted upstream from the 5′-end of GLRaV-2 CP ORF. The resulting cDNA fragment was cloned into p35S5′-BR-3′LR-Rib using Rsr II (nt 10,821) and Bst EII (nt 14,842) sites to generate the full-length GLRaV-2 cDNA clone p35S-LR-GFP or LR-GFP for the brevity.

Generation of the modified and mutant GLRaV-2 variants

The minireplicon variant mLR-GFP/GUS was engineered by modifying the LR-GFP cDNA via deletion of the cDNA fragments from the start codon of the p6 ORF (Fig. 1A) to nt 14,185 and from the Fse I site at the 3′-end of the GFP ORF to nt 15,285 (nt numbers correspond to the original GLRaV-2 cDNA). As a result, GLRaV-2 ORFs encoding p6, Hsp70h, p63, CPm, CP and p19 were deleted (Fig. 1A). The GFP ORF was then replaced with a hybrid GFP/GUS ORF described earlier (Peng et al., 2002) using Pac I at the 5′-terminus of the GFP ORF and Fse I at the 3′-terminus of the GUS ORF.

Two plasmids, pGEM-35SLR-Pro and pGEM-SP6LR-Pro, containing the whole L1 and L2 coding region and a fragment of the methyltransferase coding region (nts 1–3071) were generated by cloning the corresponding PCR-amplified fragments (Fig. 1B) into pGEM-3Zf(+). Both pGEM-35SLR-Pro and pGEM-SP6LR-Pro were used to generate pGEM-35SLR-L2$_{HA}$ and pGEM-SP635SLR-L2$_{HA}$ by inserting three copies of the hemagglutinin epitope (HA) tag (YPYDVPDYA) coding sequence downstream from codon 663 within L2 coding region. Each of these plasmids was used to introduce the following mutations into the L1 or L2.

Mutation 1 (M1) was generated by replacing the catalytic Cys$_{493}$ residue of L1 with Ala using site-directed mutagenesis. Analogously, mutation 2 (M2) was obtained via substitution of Ala for Cys$_{767}$ of L2. In ΔL2 mutation, the entire L2-coding region was deleted and Lys$_{848}$ residue downstream from L2 scissile bond was replaced with Gly to regenerate an authentic L1 cleavage site. Mutation ΔL1 was made by deleting the entire L1 coding region except for the 5′-terminal start codon. In mutation ΔNTD1, the entire N-terminal, non-proteolytic region of L1 was deleted, again except for the start codon. In mutation ΔPro1, the C-terminal proteinase domain of L1 was deleted while the N-terminal region of L1 was fused to the N-terminal region of L2. In the last mutation ΔL1/2, both L1 and L2 were deleted except for the start codon that was fused with the first Lys codon of the GLRaV-2 replicase, resulting in the formation of a replicase that differed from the proteolytically processed, wild-type replicase only by the presence of the N-terminal Met. The diagrams of all mutations are shown in Fig. 1B.

The pGEM-SP6LR-L2$_{HA}$ variants were used to analyze the proteolytic activity of the mutated proteases *in vitro*. The DNA fragments from the mutant derivatives of pGEM-35SLR-L2$_{HA}$ were cloned into mLR-GFP/GUS using Sbf I (located in the vector part of the plasmid) and Stu I (nt 3063) sites. The DNA fragments from mutant derivatives of p35S-miniV94-GFPGUS were also cloned into the full-length cDNA clone LR-GFP using Sfi I (located in the vector part of the plasmid) and Bbv CI (nt 6282).

Mutation analysis of the proteolytic activity of L1 and L2

The pGEM-SP6LR-L2$_{HA}$ variants were linearized using Sma I and the corresponding *in vitro* RNA transcripts were generated using mMessage Machine kit (Ambion). To assay the proteolytic activity of the leader proteases, the resulting capped RNA transcripts were translated using the wheat germ extracts (Promega) and [^{35}S]-Met (Amersham/Pharmacia Biotech) or a non-labeled amino acid mixture. After 1 h of incubation at 25°C, the products were separated by PAGE, electroblotted onto a PROTRAN nitrocellulose membrane and used for autoradiography or for immunoblotting using anti-HA rat monoclonal antibody (Roche) as first antibody and goat anti-rat-peroxidase as secondary antibody.

Mutation analysis of the L1 and L2 roles in RNA accumulation

Agrobacterium tumefaciens strain C58 GV2260 was transformed by each of the mLR-GFP/GUS variants by electroporation. Corresponding cultures were grown overnight at 28°C with shaking, spun down and resuspended in a buffer containing 10 mM MES-KOH (pH 5.85), 10 mM

$MgCl_2$, and 150 mM acetosyringone. Bacterial suspensions of each variant were mixed with corresponding cultures transformed to express an RNAi suppressor P1/HC-Pro from *Turnip mosaic virus* to enhance minireplicon infectivity (Chiba et al., 2006). The final bacterial concentrations were 1.0 OD_{600} for minireplicon-expressing variants and 0.1 OD_{600} for the P1/HC-Pro-expressing variant. The induced bacterial cultures were infiltrated into lower surface of the *N. benthamiana* leaves using a syringe without a needle or vacuum infiltrated into the grapevine leaves. The GFP-fluorescent leaf cells were visualized using epifluorescent stereomicroscope Leica MZ 16F (Deerfield, IL) at 8 days post-infiltration. Samples for GUS assays were prepared and GUS activity was measured using Hoefer TKO100 DNA fluorimeter (Hoefer Scientific Instruments) as described (Dolja et al., 1992).

Analysis of the local and systemic virus transport

To assay the cell-to-cell movement of the GFP-tagged virus variants, virions were isolated from the agroinfiltrated leaves of *N. benthamiana* at 2 weeks post-inoculation (Napuli et al., 2000), resuspended in a buffer containing 20 mM sodium phosphate (pH 7.4) and 1 mM Na_2-EDTA and inoculated manually to leaves of *N. benthamiana*. The fluorescent infection foci were analyzed using the epifluorescent stereomicroscope at 8 days post-inoculation.

To investigate the systemic spread in *N. benthamiana*, plasmids carrying the corresponding variants in a context of the LR-GFP were mobilized into *A. tumefaciens*, the resulting bacterial suspensions were mixed with those engineered to express P1/HC-Pro as described above, and infiltrated into leaves of young *N. benthamiana* (6–8 leaf stage) plants. After 3, 4, or 5 weeks, the upper leaves of these plants were screened for the symptom development, whereas epifluorescence microscopy and a spot camera MicroPublisher3.3 RTV (QImaging) were used to document accumulation of the virus-expressed GFP. Immunoblotting and custom-made GLRaV-2-specific antiserum in 1:5000 dilution were used to document accumulation of CP.

Virion analyses

To determine if HA-tagged L2 was associated with the virions, the sucrose gradient fractionation followed by immunoblotting was used. Virions isolated as described above were resuspended in a buffer containing 20 mM Na-phosphate (pH 7.4) and 1 mM Na_2-EDTA, loaded to the top of 10–40% sucrose gradients prepared in the same buffer, and centrifuged at 25,000 RPM for 4 h in a Beckman SW40 rotor at 4°C. Gradients were separated into 25 fractions and the immunoblot analysis was done using anti-HA rat monoclonal antibody (Roche) and GLRaV-2-specific antibody to detect $L2_{HA}$ and CP, respectively. The immunogold-specific electron microscopy to detect $L2_{HA}$ was done essentially as described (Medina et al., 1999).

Acknowledgments

The authors are thankful to Robert R. Martin and Karen Keller (USDA-ARS, Corvallis, Oregon), Baozhong Meng (University of Guelph, Ontario, Canada), Dariusz E. Goszczynski (Plant Protection Research Institute, Pretoria, South Africa), and Alexey I. Prokhnevsky (Oregon State University) for their help and advice at the initial phase of this work. Presented research was supported by contract with Growers Research Group, L.L.C. (Soledad, California) and BARD award No. IS-3784-05 to V.V.D.

References

Agranovsky, A.A., Lesemann, D.E., Maiss, E., Hull, R., Atabekov, J.G., 1995. "Rattlesnake" structure of a filamentous plant RNA virus built of two capsid proteins. Proc. Natl. Acad. Sci. U.S.A. 92 (7), 2470–2473.

Alzhanova, D.V., Hagiwara, Y., Peremyslov, V.V., Dolja, V.V., 2000. Genetic analysis of the cell-to-cell movement of beet yellows *Closterovirus*. Virology 268 (1), 192–200.

Alzhanova, D.V., Napuli, A., Creamer, R., Dolja, V.V., 2001. Cell-to-cell movement and assembly of a plant *Closterovirus*: roles for the capsid proteins and Hsp70 homolog. EMBO J. 20, 6997–7007.

Alzhanova, D.V., Prokhnevsky, A.I., Peremyslov, V.V., Dolja, V.V., 2007. Virion tails of Beet yellows virus: coordinated asembly by three structural proteins. Virology 359, 220–226.

Barrett, A.J., Rawlings, N.D., 2001. Evolutionary lines of cysteine peptidases. Biol. Chem. 382, 727–733.

Boyko, V.P., Karasev, A.V., Agranovsky, A.A., Koonin, E.V., Dolja, V.V., 1992. Coat protein gene duplication in a filamentous RNA virus of plants. Proc. Natl. Acad. Sci. U.S.A. 89, 9156–9160.

Chiba, M., Reed, J.C., Prokhnevsky, A.I., Chapman, E.J., Mawassi, M., Koonin, E.V., Carrington, J.C., Dolja, V.V., 2006. Diverse suppressors of RNA silencing enhance agroinfection by a viral replicon. Virology 346, 7–14.

de los Santos, T., de Avila Botton, S., Weiblen, R., Grubman, M.J., 2006. The leader proteinase of foot-and-mouth disease virus inhibits the induction of beta interferon mRNA and blocks the host innate immune response. J. Virol. 80, 1906–1914.

Ding, S.W., Voinnet, O., 2007. Antiviral immunity directed by small RNAs. Cell 130, 413–426.

Dolja, V.V., 2003. Beet yellows virus: the importance of being different. Mol. Plant Pathol. 4, 91–98.

Dolja, V.V., McBride, H.J., Carrington, J.C., 1992. Tagging of plant potyvirus replication and movement by insertion of beta-glucuronidase into the viral polyprotein. Proc. Natl. Acad. Sci. U.S.A. 89, 10208–10212.

Dolja, V.V., Kreuze, J.F., Valkonen, J.P., 2006. Comparative and functional genomics of closteroviruses. Virus Res. 117, 38–51.

Dougherty, W.G., Semler, B.L., 1993. Expression of virus-encoded proteinases: functional and structural similarities with cellular enzymes. Microbiol. Rev. 57 (4), 781–822.

Folimonov, A.S., Folimonova, S.Y., Bar-Joseph, M., Dawson, W.O., 2007. A stable RNA virus-based vector for citrus trees. Virology 368 (1), 205–216.

Gabrenaite-Verkhovskaya, R., Andreev, I.A., Kalinina, N.O., Torrance, L., Taliansky, M.E., Mäkinen, K., 2008. Cylindrical inclusion protein of potato virus A is associated with a subpopulation of particles isolated from infected plants. J. Gen. Virol. 89, 829–838.

Goodin, M.M., Zaitlin, D., Naidu, R.A., Lommel, S.A., 2008. *Nicotiana benthamiana*: its history and future as a model for plant–pathogen interactions. Mol. Plant Microbe. Interact. 21, 1015–1026.

Gorbalenya, A.E., Donchenko, A.P., Blinov, V.M., Koonin, E.V., 1989. Cysteine proteases of positive strand RNA viruses and chymotrypsin-like serine proteases. A distinct protein superfamily with a common structural fold. FEBS Lett. 243, 103–114.

Gorbalenya, A.E., Koonin, E.V., Lai, M.M., 1991. Putative papain-related thiol proteases of positive-strand RNA viruses. Identification of rubi- and aphthovirus proteases and delineation of a novel conserved domain associated with proteases of rubi-, alpha- and coronaviruses. FEBS Lett. 288 (1–2), 201–205.

Gorbalenya, A.E., Enjuanes, L., Ziebuhr, J., Snijder, E.J., 2006. Nidovirales: evolving the largest RNA virus genome. Virus Res 117 (1), 17–37.

Goszczynski, D.E., Kasdorf, G.G.F., Pietersen, G., van Tonder, H., 1996. Detection of two strains of grapevine leafroll-associated virus 2. Vitis 35, 133–135.

Hagiwara, Y., Peremyslov, V.V., Dolja, V.V., 1999. Regulation of *closterovirus* gene expression examined by insertion of a self-processing reporter and by northern hybridization. J. Virol. 73, 7988–7993.

Haseloff, J., Siemering, K.R., Prasher, D.C., Hodge, S., 1997. Removal of a cryptic intron and subcellular localization of green fluorescent protein are required to mark transgenic *Arabidopsis* plants brightly. Proc. Natl. Acad. Sci. U.S.A. 94 (6), 2122–2127.

Karasev, A.V., 2000. Genetic Diversity and Evolution of Closteroviruses. Annu. Rev. Phytopathol. 38, 293–324.

Karasev, A.V., Boyko, V.P., Gowda, S., Nikolaeva, O.V., Hilf, M.E., Koonin, E.V., Niblett, C.L., Cline, K., Gumpf, D.J., Lee, R.F., Garnsey, S.M., Lewandowski, D.J., Dawson, W.O., 1995. Complete sequence of the citrus tristeza virus RNA genome. Virology 208, 511–520.

Kasschau, K.D., Cronin, S., Carrington, J.C., 1997. Genome amplification and long-distance movement functions associated with the central domain of tobacco etch potyvirus helper component-proteinase. Virology 228 (2), 251–262.

Koonin, E.V., Dolja, V.V., 1993. Evolution and taxonomy of positive-strand RNA viruses: implications of comparative analysis of amino acid sequences. Crit. Rev. Biochem. Mol. Biol. 28 (5), 375–430.

Koonin, E.V., Dolja, V.V., 2006. Evolution of complexity in the viral world: the dawn of a new vision. Virus Res. 117, 1–4.

Lakatos, L., Csorba, T., Pantaleo, V., Chapman, E.J., Carrington, J.C., Liu, Y.P., Dolja, V.V., Calvino, L.F., Lopez-Moya, J.J., Burgyan, J., 2006. Small RNA binding is a common strategy to suppress RNA silencing by several viral suppressors. EMBO J. 25, 2768–2780.

Lindner, H.A., 2007. Deubiquitination in virus infection. Virology 362, 245–256.

Lu, R., Folimonov, A.S., Shintaku, M., Li, W.X., Falk, B.W., Dawson, W.O., Ding, S.W., 2004. Three distinct suppressors of RNA silencing encoded by a 20-kb viral RNA genome. Proc. Natl. Acad. Sci. U.S.A. 101, 15742–15747.

Martelli, G.P., Adams, M.J., Kreuze, J.F., Dolja, V.V., 2007. Family Flexiviridae: a case study in virion and genome plasticity. Annu. Rev. Phytopathol. 45, 73–100.

Medina, V., Peremyslov, V.V., Hagiwara, Y., Dolja, V.V., 1999. Subcellular localization of the HSP70-homolog encoded by beet yellows *Closterovirus*. Virology 260 (1), 173–181.

Meng, B., Li, C., Goszczynski, D.E., Gonsalves, D., 2005. Genome sequences and structures of two biologically distinct strains of Grapevine leafroll-associated virus 2 and sequence analysis. Virus Genes 31, 31–41.

Napuli, A.J., Falk, B.W., Dolja, V.V., 2000. Interaction between HSP70 homolog and filamentous virions of the Beet yellows virus. Virology 274 (1), 232–239.

Napuli, A.J., Alzhanova, D.V., Doneanu, C.E., Barofsky, D.F., Koonin, E.V., Dolja, V.V., 2003. The 64-kDa capsid protein homolog of beet yellows virus is required for assembly of virion tails. J. Virol. 77, 2377–2384.
Ng, J.C.K., Falk, B.W., 2006. Virus–vector interactions mediating nonpersistent and semipersistent transmission of plant viruses. Annu. Rev. Phytopathol. 44, 183–212.
Peng, C.W., Dolja, V.V., 2000. Leader proteinase of the beet yellows *Closterovirus*: mutation analysis of the function in genome amplification. J. Virol. 74, 9766–9770.
Peng, C.W., Peremyslov, V.V., Mushegian, A.R., Dawson, W.O., Dolja, V.V., 2001. Functional specialization and evolution of leader proteinases in the family Closteroviridae. J. Virol. 75 (24), 12153–12160.
Peng, C.W., Peremyslov, V.V., Snijder, E.J., Dolja, V., 2002. A replication-competent chimera of the plant and animal viruses. Virology 294, 75–84.
Peng, C.W., Napuli, A.J., Dolja, V.V., 2003. Leader proteinase of the beet yellows virus functions in long-distance transport. J. Virol. 77, 2843–2849.
Peremyslov, V.V., Dolja, V.V., 2007. Cloning of large positive-strand RNA viruses. Curr. Protocols Microbiol. (Suppl. 7), 16F.1.1–16F.1.26.
Peremyslov, V.V., Hagiwara, Y., Dolja, V.V., 1998. Genes required for replication of the 15.5-kilobase RNA genome of a plant *Closterovirus*. J. Virol. 72, 5870–5876.
Peremyslov, V.V., Hagiwara, Y., Dolja, V.V., 1999. HSP70 homolog functions in cell-to-cell movement of a plant virus. Proc. Natl. Acad. Sci. U.S.A. 96, 14771–14776.
Peremyslov, V.V., Andreev, I.A., Prokhnevsky, A.I., Duncan, G.H., Taliansky, M.E., Dolja, V.V., 2004a. Complex molecular architecture of beet yellows virus particles. Proc. Natl. Acad. Sci. U.S.A. 101, 5030–5035.
Peremyslov, V.V., Pan, Y.-W., Dolja, V.V., 2004b. Movement protein of a *Closterovirus* is a type III integral transmembrane protein localized to the endoplasmic reticulum. J. Virol. 78, 3704–3709.
Pogue, G.P., Lindbo, J.A., Garder, S.J., Fitzmaurice, W.P., 2002. Making an ally from an enemy: plant virology and the new agriculture. Annu. Rev. Phytopathol. 40, 45–74.
Prokhnevsky, A.I., Peremyslov, V.V., Napuli, A.J., Dolja, V.V., 2002. Interaction between long-distance transport factor and Hsp70-related movement protein of beet yellows virus. J. Virol. 76, 11003–11011.
Reed, J.C., Kasschau, K.D., Prokhnevsky, A.I., Gopinath, K., Pogue, G.P., Carrington, J.C., Dolja, V.V., 2003. Suppressor of RNA silencing encoded by beet yellows virus. Virology 306, 203–209.
Satyanarayana, T., Gowda, S., Mawassi, M., Albiach-Marti, M.R., Ayllon, M.A., Robertson, C., Garnsey, S.M., Dawson, W.O., 2000. *Closterovirus* encoded HSP70 homolog and p61 in addition to both coat proteins function in efficient virion assembly. Virology 278 (1), 253–265.
Satyanarayana, T., Gowda, S., Ayllon, M.A., Dawson, W.O., 2004. *Closterovirus* bipolar virion: evidence for initiation of assembly by minor coat protein and its restriction to the genomic RNA 5′ region. Proc. Natl. Acad. Sci. U.S.A. 101, 799–804.
Segers, G.C., van Wezel, R., Zhang, X., Hong, Y., Nuss, D.L., 2006. Hypovirus papin-like protease p29 suppresses RNA silencing in the natural fungal host and in a heterologous plant system. Eukaryot. Cell 5, 896–904.
Susaimuthu, J., Tzanetakis, I.E., Gergerich, R.C., Martin, R.R., 2008. A member of a new genus in the Potyviridae infects Rubus. Virus Res. 131, 145–151.
Tian, T., Rubio, L., Yeh, H.-H., Crawford, B., Falk, B.W., 1999. Lettuce infectious yellows virus: in vitro acquisition analysis using partially purified virions and the whitefly, *Bemisia tabaci*. J. Gen. Virol. 80, 1111–1117.
Tijms, M.A., Nedialkova, D.D., Zevenhoven-Dobbe, J.C., Gorbalenya, A.E., Snijder, E.J., 2007. Arterivirus subgenomic mRNA synthesis and virion biogenesis depend on the multifunctional nsp1 autoprotease. J. Virol. 81, 10496–10505.
Torrance, L., Andreev, I.A., Gabrenaite-Verhovskaya, R., Cowan, G., Makinen, K., Taliansky, M.E., 2005. An unusual structure at one end of potato potyvirus particles. J. Mol. Biol. 357, 1–8.
Tzanetakis, I.E., Martin, R.R., 2007. Strawberry chlorotic fleck: identification and characterization of a novel *Closterovirus* associated with the disease. Virus Res. 124, 88–94.
Tzanetakis, I.E., Postman, J., Martin, R.R., 2005. Characterization of a novel member of the family Closteroviridae from *Mentha* spp. Phytopathology 95, 1043–1048.
Tzanetakis, I.E., Halgren, A., Mosier, N., Martin, R.R., 2007. Identification and characterization of Raspberry mottle virus, a novel member of the Closteroviridae. Virus Res. 127, 26–33.
Urcuqui-Inchima, S., Haenni, A.L., Bernardi, F., 2001. Potyvirus proteins: a wealth of functions. Virus Res. 74, 157–175.
Valli, A., Martín-Hernández, A.M., López-Moya, J.J., García, J.A., 2006. RNA silencing suppression by a second copy of the P1 serine protease of Cucumber vein yellowing ipomovirus (CVYV), a member of the family Potyviridae that lacks the cysteine protease HCPro. J. Virol. 80, 10055–10063.
van den Born, E., Omelchenko, M.V., Bekkelund, A., Leihne, V., Koonin, E.V., Dolja, V.V., Falnes, P.O., 2008. Viral AlkB proteins repair RNA damage by oxidative demethylation. Nucleic Acids Res. 36, 5451–5461.
Xiang, C., Han, P., Lutziger, I., Wang, K., Oliver, D.J., 1999. A mini binary vector series for plant transformation. Plant Mol. Biol. 40, 711–717.
Zhu, H.Y., Ling, K.S., Goszczynski, D.E., McFerson, J.R., Gonsalves, D., 1998. Nucleotide sequence and genome organization of grapevine leafroll-associated virus-2 are similar to beet yellows virus, the *Closterovirus* type member. J. Gen. Virol. 79, 1289–1298.
Ziebuhr, J., Schelle, B., Karl, N., Minskaia, E., Bayer, S., Siddell, S.G., Gorbalenya, A.E., Thiel, V., 2007. Human coronavirus 229E papain-like proteases have overlapping specificities but distinct functions in viral replication. J. Virol. 81, 3922–3932.
Ziebuhr, J., Snijder, E.J., Gorbalenya, A.E., 2000. Virus-encoded proteinases and proteolytic processing in the Nidovirales. J. Gen. Virol. 81, 853–879.